PROCEEDINGS OF SCIENCE

MEASURING THE PHASE BETWEEN STRONG AND EM J/ψ DECAY AMPLITUDES

M. Destefanis[∗†]
Università degli Studi di Torino and INFN
E-mail: marco.destefanis@to.infn.it

QCD is certainly a well established theory describing strong interactions. Yet several physics topics which could be investigated with modern facilities can still offer various test of this theory. The investigation of the kinematic region near J/ψ production can provide a check of the QCD perturbative approach. In this energy range, an interference between the resonant $e^+e^- \to J/\psi \to$ hadrons and the non-resonant $e^+e^- \to$ hadrons amplitudes can in principle occur. A perturbative approach suggests that those amplitudes are expected to be all almost real, i.e. the relative phase between the above cited amplitudes is expected to be $0^\circ/180^\circ$, depicting hence the full interference scenario. Nevertheless, data available in the literature concordantly suggest a relative phase of 90° and, hence, the no interference scenario. An experimental approach able to provide a measurement of the relative phase in a model independent way, and in particular its deployment in the BESIII scenario, will be discussed in details.

XXI International Baldin Seminar on High Energy Physics Problems,
September 10-15, 2012
JINR, Dubna, Russia

∗Speaker.
†For the BESIII Collaboration.

PoS(Baldin ISHEPP XXI)031

1. Relative phase measurement

The energy region close to the J/ψ peak can provide unique opportunities to investigate strong and electromagnetic interactions and to probe the QCD perturbative approach and its limits in this energy range.

An energy scan below the J/ψ peak may reveal an interference between the resonant $e^+e^- \to J/\psi \to hadrons$ and non-resonant $e^+e^- \to hadrons$ amplitudes. The relative phase between the strong and the electromagnetic amplitudes could be investigated in a model independent way by searching for an interference at different Q^2 values. The relatively small J/ψ decay width ($\simeq$93 KeV) is often interpreted as a proof that the perturbative regime holds. In this regime the J/ψ resonant amplitudes, the strong A_{3g} (Fig. 1a) and the electromagnetic A_γ (Fig. 1b) ones, are expected to be almost real [1], as the non resonant electromagnetic amplitude A_{EM} (Fig. 1c).

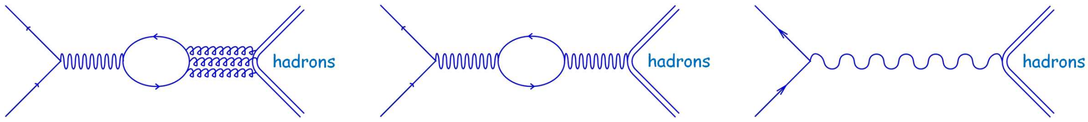

(a) **(b)** **(c)**

Figure 1: *Diagram for the process $e^+e^- \to hadrons$: **(a)** strong A_{3g}, **(b)** electromagnetic A_γ, and **(c)** non resonant A_{EM} contributions.*

In such a scenario, i.e. with a relative phase of $\sim 0°/180°$, an interference between the three above described amplitudes should occur. On the contrary, the experimental data available in the literature suggest an unexpected relative phase close to $\sim 90°$: the different investigated J/ψ decays into $N\bar{N}$, VP, PP, and VV (where N, V and P stand for nucleon, vector and pseudo-scalar meson respectively), show all no-interference patterns [1, 2, 3, 4, 5, 6]. The $J/\psi \to N\bar{N}$ decay is well suited for such kind of studies, since the three gluons match the three $q\bar{q}$ pairs of the nucleon. In particular, the BESIII Collaboration [7] has measured the branching ratios of J/ψ decays into $p\bar{p}$ and $n\bar{n}$, which should be sensitive to an interference pattern: the two branching ratios are quite similar, pointing toward a no-interference scenario, and leading to an estimated relative phase of $88.1° \pm 8.1°$ [6]. QCD calculations so far could not explain such a relevant relative phase.

An interference pattern was observed in an earlier stage and in leptonic final states by SPEAR[8] and BESII[9]. In both scenarios inclusive set of final states provided no indication of an interference, but, as soon as exclusive final states were considered, the dips in the cross sections could be detected. Since in inclusive measurements the interference patterns are expected to vanish, the only feasible approach requires an inclusive set of different exclusive measurements.

Among the possible exclusive final states, we focused on $e^+e^- \to p\bar{p}$, $e^+e^- \to \rho\pi$, and $e^+e^- \to 5\pi$. These final states were chosen to explore different experimental scenarios, since they are characterised by significantly different branching ratios and cross sections in the non-resonant "continuum" region (the energy region in the 3 GeV range far from the J/ψ peak), and since they have been widely investigated up to now. Moreover, there are also other final states which are under investigation and have already been discussed in the litterature [10].

The BESIII experimental scenario profits of the excellent performances of the BEijing Spectrometer, already in its third hardware configuration after the previous upgrade from BES to BESII;

the spectrometer is hosted on the BEPCII, the e^+e^- collider set at the Institute of High Energy Physics (IHEP) in Beijing. Fig. 2 shows a 3D view of the spectrometer. The $\sqrt{s}$ of the collisions can be tuned according to the required center of mass energy, in order to produce different charmonium resonances as for example J/ψ, ψ' or ψ''. The investigation of charmonium states and spectroscopy studies have a prominent role in the wide BESIII physics program [7]. The Beijing

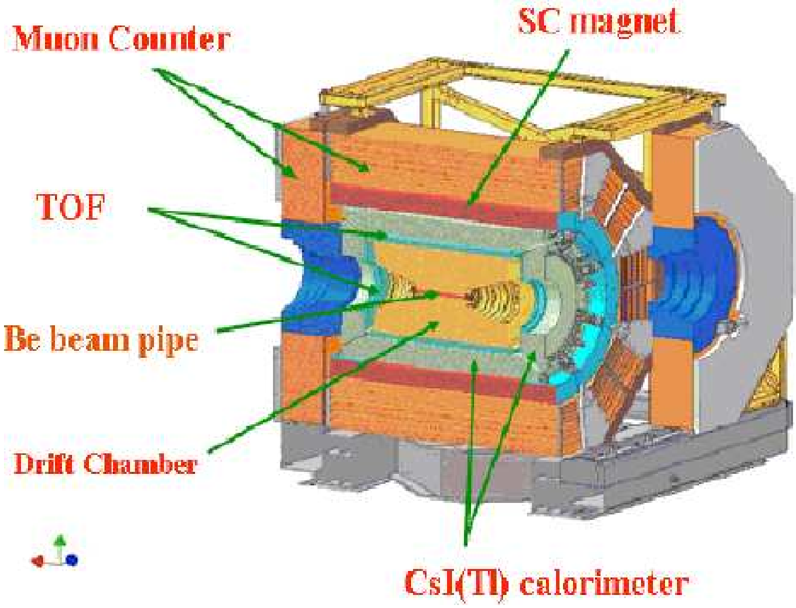

Figure 2: *3D view of the BESIII spectrometer.*

Electron-Positron Collider II (BEPCII) is designed to provide an instant Luminosity up to 10^{33} $cm^{-2}s^{-1}$ with beam currents up to 0.93 A and beam momenta up to 2.3 GeV/c. The BESIII spectrometer is characterised a wide geometrical acceptance, 93% of 4π, and by a shell like structure: departing from the interaction point, it hosts 43 small-celled, helium-based main drift chamber (MDC) chambers, a time-of-flight system (TOF) for particle identification, and an electromagnetic calorimeter (EMC) composed of 6240 CsI (Tl) crystals arranged in a cylindrical shape (barrel) plus two end-caps; these three detectors are operating inside a 1T solenoidal magnetic field. The magnet iron yoke includes a muon chamber system composed of 1000 m^2 resistive plate chambers arranged in 9 layers in the barrel and 8 layers in the end-caps. A Zero Degree Detector (ZDD) was installed on August 2011 for Initial State Radiations (ISR) studies.

In the procedure adopted in the presented investigation, both for the generated cross section and for the fitting procedure, the initial state initial state radiation, crucial when considering e^+e^- interactions, are accounted for. The cross section

$$\sigma[nb] = 12\pi B_{in}B_{out}\left[\frac{\hbar c}{W}\right]^2 \cdot 10^7 \cdot \left|\frac{C_1 + C_2 e^{i\varphi}}{W - W_{ris} + i\Gamma/2} + C_3 e^{i\varphi}\right|^2, \tag{1.1}$$

has been assumed for both event generation and fitting procedure. In such a simple model, the radiation has been limited to 300 MeV, a conservative assumption, since accounts as almost 20% of the E_{CM}. A beam energy spread of 0.92 MeV has been taken into account as well. Fig. 3

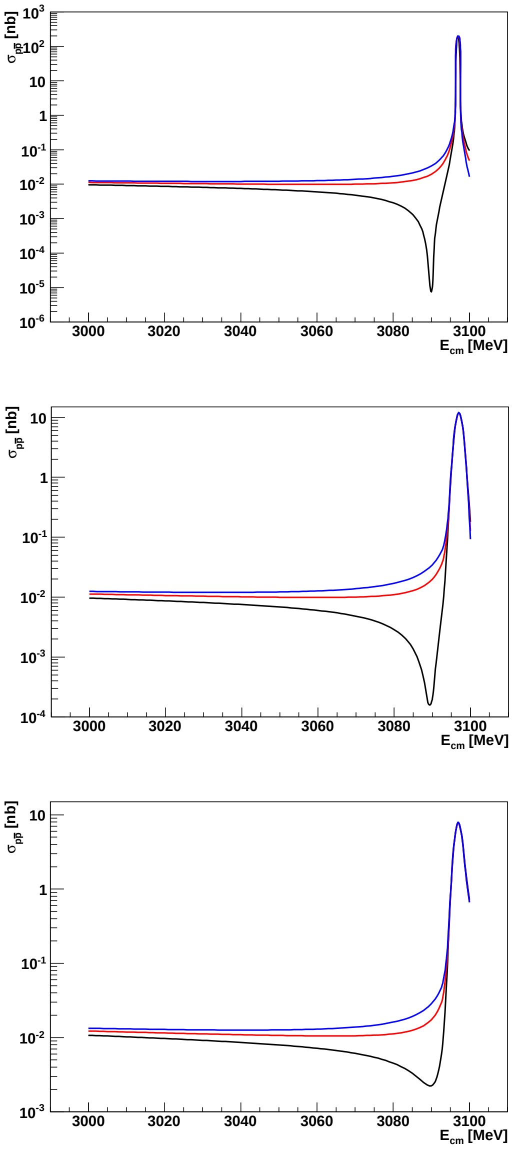

Figure 3: Effects of beam spread and initial state radiation on the simulated cross section in the case of: a) no corrections; b) beam spread corrections only; c) beam spread plus initial state radiation. The maximum interference, 0° (black) and 180° (blue), and the no interference, 90° (red), scenarios are here presented.

shows the combined effects of the beam spread and of the initial state radiation to the cross section: an evident broadening of the J/ψ peak and of the dip. Although the final optimization has been performed in the case of the process $e^+e^- \to p\bar{p}$ only, the reconstruction of the phase has been evaluated for all the above mentioned processes.

The selection of the energy points needed for a line shape scan leading to an effective determination of the relative phase has been performed considering as the maximum interference scenario a relative phase $\Delta\varphi = 0°$ and as the no interference scenario a $\Delta\varphi = 90°$.

To investigate the maximum interference scenario two points at low energy values (low W)

are needed to anchor the cross section to the continuum (the cross section value far from the J/ψ resonance) and to its slope. Two more energy points have been chosen in correspondence of the cross section dip for the $e^+e^- \to p\bar{p}$ and $e^+e^- \to \rho\pi$ processes. A fifth point has been chosen at the beginning of the Breit-Wigner, where the resonant amplitudes should start to dominate the $e^+e^- \to p\bar{p}$ process.

The literature suggest a no interference scenario; the gradient of $\Delta\varphi$ = 90° $[(\sigma_{90} - \sigma_i)/\sigma_{90}]$ has hence been calculated for different φ values. The proposed measurement is more sensible for maximum/minimum values of the gradient, that correspond roughly to the position of the cross section dip. Thus the selected energy points has been: 3050, 3060, 3083, 3090, and 3093 MeV.

In order to take into account the initial state radiation of the two colliding particles, the cross section at each energy point has been obtained by a Monte-Carlo simulation of 100000 events. The rate at each energy point has then been smeared with a Gaussian distribution centered in the simulated point with a sigma equal to the the rate error. The Gaussians at the selected energy points have then been considered by the fitting routine to attempt the fit. To define the precision of our parameters this procedure has been iterated 100 times, so that the precision could be obtained propagating the standard error of the cross sections.

The rates at each energy point and hence our proposed measurements depend heavily on the collected integrated Luminosity per point. We have assumed to dedicate one full day of data taking to each energy point, i.e. a total of five days of beam time; the integrated Luminosity expected for each point has been determined assuming an injection efficiency of 0.8, and a reconstruction efficiency for a selection of the different channels under investigation: 0.67, 0.38, and 0.20 for $p\bar{p}$, $\rho\pi$, and 5π respectively.

The precision of the fit increases with the square root of the integrated Luminosity. Fig. 4 shows the precision plotted as function of the integrated Luminosity for different assumptions of the relative phase for the $p\bar{p}$ and the $\rho\pi$ processes. The sensitivity is lower for larger relative phase values; this is due to the missing symmetry between the angular regions 0°-90° and 90°-180°, as shown by Fig. 3.

The precision of the relative phase measurement has shown a rather weak sensitivity on how the total integrated luminosity is shared between the different energy points. We have hence selected the more conservative option for the lumiosity ratio: 1:1:1:1:1, i.e. the same Luminosity. Assuming a Luminosity of $2{\cdot}10^{32}$ [cm^{-2}s^{-1}], an integrated Luminosity of 14pb^1 has been requested for each energy point.

One more energy point is needed to have a stable fitting procedure with three free parameters: $\Delta\varphi$, the relative phase, σ_{cont}, the cross section at the continuum, B$_{out}$, the branching ratio. A large integrated Luminosity had been already collected during previous data taking runs at the J/ψ peak; such a point has hence been added to the above described five points set.

Systematic uncertainties for the $e^+e^- \to p\bar{p}$ process have been estimated according to [6], and rescaled considering the lower considered cross sections. They are not sizeable, and to be more conservative they have been directly added to the estimated statistical uncertainties, rather then considering the usual global uncertainties evaluation procedure.

Data in the literature point toward a $\Delta\varphi \sim 90°$; the overall uncertainties obtained in such a scenario are quoted in Table 1. The statistical significance is good enough to discriminate between different theoretical predictions.

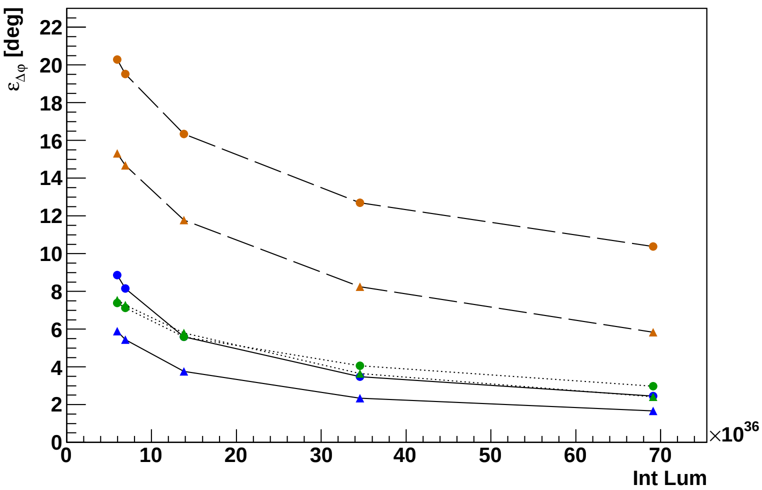

Figure 4: *Precision ($\varepsilon_{\Delta\varphi}$) plotted as function of the integrated Luminosity ([cm^{-2}]) for the $p\bar{p}$ (circles) and $\rho\pi$ (triangles) final states and for different relative phases: 10° (dotted line), 90° (full line), and 170° (dashed line).*

$\Delta\varphi$ [°]	$\Delta\sigma$ [pb]	$\Delta B_{out}/B_{out}$
6.1	0.9	$2{\cdot}10^{-3}$

Table 1: Expected precisions at $\Delta\varphi = 90°$ for a three parameters fit; systematic uncertainties have been accounted for.

The required integrated Luminosities have been collected by BESIII during the 2012 data taking run, at the required beam energies. An energy point close to 3083 MeV had already been collected for other studies, and has then been included in the considered data set. The sixth point, as explained above, had already been collected during the 2011 run, with a pretty large integrated Luminosity: this point made the fit performed with three free parameters possible. Data cleaning procedures and data quality checks have been already performed, and physical analysis is ongoing.

During the 2012 BESIII data taking run more energy points, although with lower integrated Luminosities, were collected for a J/ψ resonance scan. These points could be included in the considered data set for the presented measurement and increase the precision with which the parameters can be determined.

2. Acknowledgements

This work was supported in part by Università degli Studi di Torino, Regione Piemonte, INFN Torino, and IHEP Beijing.

References

[1] R. Baldini, C. Bini, E. Luppi, Phys. Lett. B404, 362 (1997).

[2] R. Baldini et al., Phys. Lett. B444, 111 (1998).

[3] L. Kopke and N. Wermes, Phys. Rep. 174, 67 (1989).

[4] J. Jousset et al., Phys. Rev. D41,1389 (1990).

[5] M. Suzuki et al., Phys. Rev. D60, 051501 (1999).

[6] M. Ablikim et al., Phys. Rev. D 86, 032014 (2012).

[7] D.M. Asner et al, Physics at BES-III, arXiv:0809.1869v1 [hep-ex] (2008)

[8] A.M. Boyarski et al., Phys. Rev. Lett. 34, 1357 (1975).

[9] J.Z. Bai et al., Phys. Lett. B 355, 374-380 (1995).

[10] H. Czyz, and J. Kühn, Phys.Rev. D80: 034035 (2009).